Decaying Dark Energy in Light of the Latest Cosmological Dataset

Ivan de Martino [ID]

Department of Theoretical Physics and History of Science, University of the Basque Country UPV/EHU, Faculty of Science and Technology, Barrio Sarriena s/n, 48940 Leioa, Spain; ivan.demartino@ehu.eus

check for updates

Abstract: Decaying Dark Energy models modify the background evolution of the most common observables, such as the Hubble function, the luminosity distance and the Cosmic Microwave Background temperature–redshift scaling relation. We use the most recent observationally-determined datasets, including Supernovae Type Ia and Gamma Ray Bursts data, along with $H(z)$ and Cosmic Microwave Background temperature versus z data and the reduced Cosmic Microwave Background parameters, to improve the previous constraints on these models. We perform a Monte Carlo Markov Chain analysis to constrain the parameter space, on the basis of two distinct methods. In view of the first method, the Hubble constant and the matter density are left to vary freely. In this case, our results are compatible with previous analyses associated with decaying Dark Energy models, as well as with the most recent description of the cosmological background. In view of the second method, we set the Hubble constant and the matter density to their best fit values obtained by the *Planck* satellite, reducing the parameter space to two dimensions, and improving the existent constraints on the model's parameters. Our results suggest that the accelerated expansion of the Universe is well described by the cosmological constant, and we argue that forthcoming observations will play a determinant role to constrain/rule out decaying Dark Energy.

Keywords: Dark Energy; statistical analysis; Baryon Acoustic Oscillation (BAO); Supernovae; cosmological model; Hubble constant; Cosmic Microwave Background (CMB) temperature

1. Introduction

In the last decades, several observations have pointed out that the Universe is in an ongoing period of accelerated expansion that is driven by the presence of an exotic fluid with negative pressure [1–12]. Its simplest form is a cosmological constant Λ, having an equation of state $w = -1$. More complicated prescriptions lead to the so-called Dark Energy (DE). Although several models have been proposed to explain DE [13–27], the observations have only determined that it accounts for $\sim 68\%$ of the total energy-density budget of the Universe, while its fundamental nature is still unknown (see, for instance, the reviews [28,29]). In addition, we should mention that the accelerated expansion of the Universe could be explained by several modifications of the gravitational action. For example, introducing higher order terms of the Ricci curvature in the Hilbert–Einstein Lagrangian, gives rise to an effective matter stress–energy tensor which could drive the current accelerated expansion (see, for example, the reviews [12,30–35]). Another alternative for reproducing the dark energy effects is by introducing non-derivative terms interactions in the action, in addition to the Einstein–Hilbert action term, such that it creates the effect of a massive graviton [36–38].

We are interested in exploring a specific decaying DE model, $\Lambda(z) \propto (1 + z)^m$, leading to creation/annihilation of photons and Dark Matter (DM) particles. The model is based on the theoretical framework developed in [39–43], while the thermodynamic features have been developed in [44,45]. Since DE continuously decays into photons and/or DM particles along the cosmic evolution,

the relation between the temperature of the Cosmic Microwave Background (CMB) radiation and the redshift is modified.

In the framework of the standard cosmological model, the Universe expands adiabatically and, as consequence of the entropy and photon number conservation, the temperature of the CMB radiation scales linearly with redshift, $\propto (1+z)$. Nevertheless, in those models where conservation laws are violated, the creation or annihilation of photons can lead to distortions in the blackbody spectrum of the CMB and, consequently, to deviations of the standard CMB temperature–redshift scaling relation. Such deviations are usually explored with a phenomenological parameterization, such as $T_{\mathrm{CMB}}(z) = T_0(1+z)^{1-\beta}$ proposed in [41], where β is a constant parameter ($\beta = 0$ means adiabatic evolution), and T_0 is the CMB temperature at $z = 0$, which has been strongly constrained with COBE-FIRAS experiment, $T_0 = 2.7260 \pm 0.0013$ K [46]. The parameter β has been constrained using two methodologies: (a) the fine structure lines corresponding to the transition energies of atoms or molecules, present in quasar spectra, and excited by the CMB photon [47]; and (b) the multi-frequency measurements of the Sunyaev-Zel'dovich (SZ) effect [48–50]. Recent results based on data released by the *Planck* satellite and the *South Pole Telescope* (SPT) have led to sub-percent constraints on β which results to be compatible with zero at 1σ level (more details can be found in [11,51–56]).

In this paper, we start with the theoretical results obtained in [44,45]. Such a model has been constrained using luminosity distance measurements from Supernovae Type Ia (SNIa), differential age data, Baryonic Acoustic Oscillation (BAO), the CMB temperature–redshift relation, and the CMB shift parameter. Since the latter depends on the redshift of the last surface scattering, $z_{CMB} \sim 1000$, it represents a very high redshift probe. On the contrary, other datasets were used to probe the Universe at low redshift, $z \lesssim 3.0$. We aim to improve those constraints performing two different analysis: first, we constrain the whole parameter space to study the possibility of the model to alleviate the tension in the Hubble constant (see Section 5.4 in [10] for the latest results on the subject); and, second, we adopt the *Planck* cosmology to improve the constraint on the remaining parameters. Thus, we retain the SNIa, and use the most recent measurements the differential age, BAO, and the CMB temperature–redshift data. In addition, we use luminosity distances data of Gamma Ray Burst (GRB), which allow us to extend the redshift range till $z \sim 8$. Finally, we also use the reduced (compressed) set of parameters from CMB constraints [10].

The paper is organized as follows. In Section 2, we summarize the theoretical framework starting from the general Friedman–Robertson–Walker (FRW) metric, and point out the modification to the cosmological background arising from the violation of the conservation laws. In Section 3, we present the datasets used in the analysis, and the methodology implemented to explore the parameter space. The results are shown and discussed in Section 4 and, finally, in Section 5, we give our conclusions.

2. Theoretical Framework

The starting point is the well-known FRW metric

$$ds^2 = c^2 dt^2 - a^2(t)\left[\frac{dr^2}{1-kr^2} + r^2(d\theta^2 + \sin^2\theta d\phi^2)\right],\tag{1}$$

where $a(t)$ is the scale factor and k is the curvature of the space time [57]. In General Relativity (GR), one obtains the following Friedman equations:

$$8\pi G(\rho_{m,tot} + \rho_x) + \Lambda_0 c^2 = 3\left(\frac{\dot{a}}{a}\right)^2 + 3\frac{kc^2}{a^2},\tag{2}$$

$$\frac{8\pi G}{c^2}(p_{m,tot} + p_x) - \Lambda_0 c^2 = -2\frac{\ddot{a}}{a} - \frac{\dot{a}^2}{a^2} - \frac{kc^2}{a^2},\tag{3}$$

where the total pressure is $p_{m,tot} = p_\gamma$, the total density is $\rho_{m,tot} = \rho_m + \rho_\gamma$, and ρ_x and p_x are the density and pressure of DE, respectively. Following [44,45], we set both the "bare" cosmological constant Λ_0 and the curvature k equal to 0.

In the standard cosmology, the Bianchi identities hold and the stress–energy momentum $T^{\mu\nu}$ is locally conserved

$$\nabla_\mu T^{\mu\nu} = 0 \,. \tag{4}$$

Adopting a perfect fluid, the previous relation can recast as

$$\dot{\rho} + 3(\rho + p)H = 0 \,, \tag{5}$$

where $H \equiv \dot{a}/a$ is the definition of the Hubble parameter. Thus, each component is conserved. Nevertheless, due to the photon/matter creation/annihilation happening in the case of decaying DE, the conservation equation is recast in the following relations:

$$\dot{\rho}_m + 3\rho_m H = (1 - \epsilon)\, C_x \,, \tag{6}$$
$$\dot{\rho}_\gamma + 3\gamma\rho_\gamma H = \epsilon\, C_x \,, \tag{7}$$
$$\dot{\rho}_x + 3(p_x + \rho_x)H = -C_x \,, \tag{8}$$

where γ is a free parameter determining the equation of state of radiation $p_\gamma = (\gamma - 1)\rho_\gamma$ and, C_x and ϵ account for the decay of DE. C_x describe the physical mechanism leading to the production of particles (see, for instance, the thermogravitational quantum creation theory [40] or the quintessence scalar field cosmology [14]), and ϵ must be small enough in order to have the current density of radiation matching the observational constraints. Assuming $p_x = -\rho_x$, and defining

$$\rho_x = \frac{\Lambda(t)}{8\pi G} \,, \tag{9}$$

the parameter C_x can be obtained from the Equation (8)

$$C_x = -\frac{\dot{\Lambda}(t)}{8\pi G} \,. \tag{10}$$

Following [44,45], one can adopt a power law model

$$\Lambda(t) = B\left(\frac{a(t)}{a(0)}\right)^{-m} = B(1+z)^m \,, \tag{11}$$

then, writing Equation (2) at the present epoch, one can obtain $B = 3H_0^2(1 - \Omega_{m,0})$, where $\Omega_{m,0}$ is the matter density fraction at $z = 0$. It is very straightforward to verify that setting the power law index $m = 0$ leads to the cosmological constant. From Equation (8), it is also possible to write down an effective equation of state for the DE [45]:

$$w_{eff} = \frac{m}{3} - 1 \,. \tag{12}$$

Finally, using Equations (2) and (6)–(8), the Hubble parameter can be obtained [43–45]:

$$H(z) \simeq \frac{8\pi G}{3}(\rho_m + \rho_x) = H_0\left[\frac{3(1 - \Omega_{m,0})}{3 - m}(1+z)^m + \frac{(3\Omega_{m,0} - m)}{3 - m}(1+z)^3\right]^{1/2} \,. \tag{13}$$

Let us note that the standard Hubble parameter is recovered by setting $m = 0$ in Equation (13). Having the Hubble parameter allows us to compute the luminosity distance as follows

$$D_L = \frac{(1+z)c}{H_0} \int_0^z \frac{dz'}{E(z')},$$ (14)

where we have defined $E(z) \equiv H(z)/H_0$.

Finally, following the approach originally proposed in [39], combining the Equations (6)–(8), with the equation for the number density conservation

$$\dot{n}_\gamma + 3n_\gamma H = \psi_\gamma,$$ (15)

where ψ_γ is the photon source, and the Gibbs Law

$$n_\gamma T_\gamma d\sigma_\gamma = d\rho_\gamma - \frac{\rho_\gamma + p_\gamma}{n_\gamma} dn_\gamma,$$ (16)

one obtains, through the use of thermodynamic identities, the following CMB temperature redshift relation (see for more details [43,45]):

$$T_{CMB}(z) = T_0(1+z)^{3(\gamma-1)} \times \left(\frac{(m - 3\Omega_{m,0}) + m(1+z)^{m-3}(\Omega_{m,0} - 1)}{(m-3)\Omega_{m,0}} \right)^{(\gamma-1)}.$$ (17)

Again, setting $m = 0$ gives the standard relation $T_{CMB}(z) = T_0(1+z)$. Equations (13), (14) and (17) can be easily implemented to test the decaying DE scenario. To show the effectiveness of these observables in constraining the cosmological model, we depict in Figure 1 their scalings as a function of the redshift for different value of the parameters γ and m, while we set H_0 and Ω_0 to their best fit from *Planck* satellite. In Figure 1a–c, we fix $\gamma = 4/3$ (which represents its standard value) while varying m in the range $[-0.5, 0.5]$ to show its impact on the Hubble constant, the luminosity distance and the CMB temperature. On the contrary, in Figure 1d, we set $m = 0$ (standard value) and vary γ illustrating how much the T_{CMB}-redshift relation is affected. The redshift ranges in the panels are set to the ones of the datasets. Looking at the plots, it is clear that the data will be really sensible to a variation of γ, while m will be more difficult to constrain.
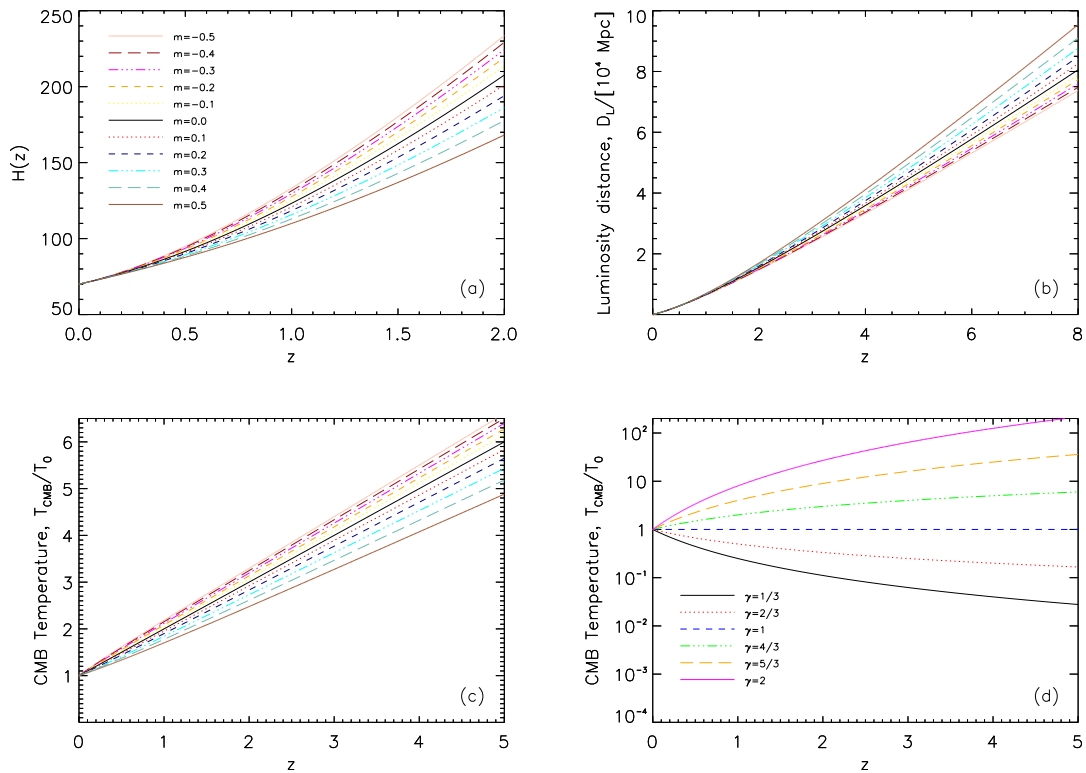
Figure 1. The figure shows as function of redshift the Hubble constant in panel (**a**), the luminosity distance in panel (**b**), and the CMB temperature in panels (**c**) and (**d**). Colors and lines indicate the different values assigned to the parameters m and γ to illustrate their impact on the observables.

3. Methodology and Data

We use measurements of $H(z)$, luminosity distances from SNIa and GRBs, BAO, and the CMB temperature–redshift relation. Then, we predict the theoretical counterparts using Equations (13), (14), and (17), and fit each one to the corresponding dataset computing the likelihood $-2\log\mathcal{L} = \chi^2(\mathbf{p})$, where $\mathbf{p} = [H_0, \Omega_{m,0}, m, \gamma]$ are the parameters of the model. The parameter space is explored using a Monte Carlo Markov Chain (MCMC) based on the Metropolis–Hastings [58,59] sampling algorithm with an adaptive step size to guarantee an optimal acceptance rate between 20% and 50% [60,61], while the convergence is ensured by the Gelman–Rubin criteria [62]. Once the convergence criteria is satisfied, the different chains are merged to compute the marginalized likelihood $\mathcal{L}(\mathbf{p}) = \Pi_k \mathcal{L}(\mathbf{p})$, where k indicates the different datasets, and to constrain the model's parameters. The priors are specified in Table 1.

Table 1. Parameter space explored by the MCMC algorithm.

Parameter	Priors
H_0	$[50.0, 100.0]$
$\Omega_{m,0}$	$[0.0, 1.0]$
m	$[-1, 1]$
γ	$[1.0, 2.0]$

Finally, the expectation value ($\langle p_i \rangle$) of the 1D marginalized likelihood distribution and the corresponding variance are computed as follows [63]

$$\langle p_i \rangle = \int d^{N_s} \mathbf{p} \, \mathcal{L}(\mathbf{p}) p_i, \tag{18}$$

$$\sigma_i^2 = \int d^{N_s} \mathbf{p} \, \mathcal{L}(\mathbf{p}) (p_i - \langle p_i \rangle)^2, \tag{19}$$

where N_s is the dimension of the parameter space.

Finally, the joint likelihood of the independent observables is used to compare decaying DE model with ΛCDM employing the Akaike Information Criteria (AIC) [64]:

$$AIC = -2 \log \mathcal{L}_{max} + 2 N_p, \tag{20}$$

where N_p is the number of parameters. A negative variation of the AIC indicator with respect to the reference model, $\Delta(AIC) = AIC_{dec.DE} - AIC_{\Lambda CDM}$, would indicate the model performs better than ΛCDM.

3.1. Supernovae Type Ia

We use a dataset of 557 Supernovae Type Ia (SNIa) in the redshift range $z = [0, 1.4]$ extracted from the UnionII catalogue (more details can be found in [65]). The observable is the so-called distance modulus μ_{obs}, which is the difference of the apparent and absolute magnitudes. Its theoretical counterpart can be computed starting from the luminosity distance in Equation (14), and it is given by

$$\mu_{th}(z) = 5 \log_{10} \hat{D}_L(z) + \mu_0, \tag{21}$$

where $\mu_0 = 42.38 - 5 \log_{10} h$, with $h \equiv H_0/100$, and $\hat{D}_L(z)$ is given by

$$\hat{D}_L(z) = (1+z) \int_0^z \frac{dz'}{E(z')}. \tag{22}$$

Then, we can define the χ^2 function as

$$-2 \log \mathcal{L}_{SN}(\mathbf{p}) = \chi^2_{SN}(\mathbf{p}) = \sum_{i=1}^{557} \left(\frac{\mu_{th}(z_i, \mathbf{p}) - \mu_{obs}(z_i)}{\sigma_\mu(z_i)} \right)^2, \tag{23}$$

where $\sigma_\mu(z)$ is the error on $\mu_{obs}(z)$. Let us note that the parameter μ_0 encodes the dependence by the Hubble constant. Whenever one is not interest in fitting H_0, the marginalized χ^2 function can be defined as [66–69]:

$$\tilde{\chi}^2_{SN}(\mathbf{p}) = \tilde{A} - \frac{\tilde{B}^2}{\tilde{C}}, \tag{24}$$

where

$$\tilde{A} = \sum_{i=1}^{557} \left(\frac{\mu_{th}(z_i, \mathbf{p}, \mu_0 = 0) - \mu_{obs}(z_i)}{\sigma_\mu(z_i)} \right)^2, \tag{25}$$

$$\tilde{B} = \sum_{i=1}^{557} \frac{\mu_{th}(z_i, \mathbf{p}, \mu_0 = 0) - \mu_{obs}(z_i)}{\sigma_\mu^2(z_i)}, \tag{26}$$

$$\tilde{C} = \sum_{i=1}^{557} \frac{1}{\sigma_\mu^2(z_i)}. \tag{27}$$

3.2. Differential Ages, $H(z)$

Following [70], we use 30 uncorrelated measurements of expansion rate, $H(z)$, that have been obtained using the differential age method [71–78]. Thus, we define the corresponding χ^2 as

$$- 2 \log \mathcal{L}_{\text{H}}(\mathbf{p}) = \chi^2_{\text{H}}(\mathbf{p}) = \sum_{i=1}^{30} \left(\frac{H(z_i, \mathbf{p}) - H_{obs,}(z_i)}{\sigma_H(z_i)} \right)^2, \tag{28}$$

where $\sigma_H(z)$ is the error on $H_{obs}(z)$. As stated in Section 3.1, the marginalized χ^2 with respect to H_0 can be also defined using Equation (24), where, for the $H(z)$ dataset, we have

$$\tilde{A} = \sum_{i=1}^{30} \left(\frac{(H(z_i, \mathbf{p}, H_0 = 1) - H_{obs}(z_i)}{\sigma_H(z_i)} \right)^2, \tag{29}$$

$$\tilde{B} = \sum_{i=1}^{30} \frac{H(z_i, \mathbf{p}, H_0 = 1) - H_{obs}(z_i)}{\sigma_H^2(z_i)}, \tag{30}$$

$$\tilde{C} = \sum_{i=1}^{30} \frac{1}{\sigma_H^2(z_i)}. \tag{31}$$

3.3. Baryonic Acoustic Oscillation

It is customary to define the BAO's observable as the following ratio: $\hat{\Xi} \equiv r_d / D_V(z)$, where r_d is the sound horizon at the drag epoch z_d [79]:

$$r_d = \int_{z_d}^{\infty} \frac{c_s(z)}{H(z)} dz, \tag{32}$$

and D_V the spherically averaged distance measure [80]

$$D_V(z) \equiv \left[(1+z)^2 d_A^2(z) \frac{cz}{H(z)} \right]^{1/3}. \tag{33}$$

Following [70], we use data from the 6dFGS [81], the SDSS DR7 [82], the BOSS DR11 [83–85], which are reported in Table I of [70]. Such a dataset is uncorrelated, therefore the likelihood can be straightforwardly computed as

$$- 2 \log \mathcal{L}_{\text{BAO}}(\mathbf{p}) = \chi^2_{\text{BAO}}(\mathbf{p}) = \sum_{i=1}^{6} \left(\frac{\hat{\Xi}(\mathbf{p}, z_i) - \Xi_{obs}(z_i)}{\sigma_\Xi(z_i)} \right)^2, \tag{34}$$

where $\sigma_\Xi(z)$ is the error on $\Xi(z)$.

3.4. Gamma Ray Burst

We use a dataset of 109 GRB given in [86] which have been already used in other cosmological analysis (see for example [87]). The dataset was compiled using the Amati relation [88–90], and it is formed by 50 GRBs at $z < 1.4$ and 59 GRBs spanning the range of redshift $[0.1, 8.1]$. As it is for SNIa, the observable is the distance modulus, which in the case of GRBs is related to peak energy and the bolometric fluence (for more details, see [86,87]). The theoretical counterpart is computed using Equation (21), and the χ^2 function is defined as follows

$$- 2 \log \mathcal{L}_{\text{GRB}}(\mathbf{p}) = \chi^2_{\text{GRB}}(\mathbf{p}) = \sum_{i=1}^{109} \left(\frac{\mu_{th}(z_i, \mathbf{p}) - \mu_{obs}(z_i)}{\sigma_\mu(z_i)} \right)^2. \tag{35}$$

3.5. T_{CMB}–Redshift Relation

The last dataset is represented by the measurements of the CMB temperature at different redshifts. We use 12 data points obtained by using multi-frequency measurements of the Sunyaev–Zel'dovich effect produced by 813 galaxy clusters stacked on the CMB maps of the *Planck* satellite [54]. To those data, we add 10 high redshift measurements obtained through the study of quasar absorption line spectra [47]. The full dataset includes 22 data points spanning the redshift range $[0.0, 3.0]$, and they are listed in Table I of [51]. Finally, we predict the theoretical counterpart using Equation (17), and we compute the likelihood as

$$-2 \log \mathcal{L}_{\mathrm{T_{CMB}}}(\mathbf{p}) = \chi^2_{\mathrm{T_{CMB}}}(\mathbf{p}) = \sum_{i=1}^{22} \left(\frac{T_{CMB,th}(z_i, \mathbf{p}) - T_{CMB,obs}(z_i)}{\sigma_{T_{CMB}}(z_i)} \right)^2. \tag{36}$$

3.6. PlanckTT + LowP

The CMB power spectrum is the most powerful tools used to constrain cosmological parameters. However, the calculation of the power spectrum is time consuming, and it is common to use the so-called reduced parameters. It is possible to compress the whole information of the CMB power spectrum into a set of four parameters [91,92]: the CMB shift parameter (R), the angular scale (l_A) of the sound horizon at the redshift of the last scattering surface (z_*), the baryon density, and the scalar spectral index. Here, we rely only on R and l_A which can be compute as follows:

$$R = \sqrt{\Omega_{m,0}} \int_0^{z_*} \frac{dz'}{E(z')}, \tag{37}$$

$$l_A = \frac{\pi D_A(z_*)}{r_s(z_*)}, \tag{38}$$

where r_s is the sound horizon at z_*. In the 2015 data release of *Planck* satellite, the observational values of those parameters are: $[R, l_A] = [1.7488; 301.76] \pm [0.0074; 0.14]$ (for more details see Section 5.1.6 in [93]). Thus, the likelihood can be straightforwardly computed as

$$-2 \log \mathcal{L}_{\mathrm{CMB}}(\mathbf{p}) = \chi^2_{\mathrm{CMB}}(\mathbf{p}) = \left(\frac{R_{obs} - R_{th}(\mathbf{p})}{\sigma_R} \right)^2 + \left(\frac{l_{A,obs} - l_{A,th}(\mathbf{p})}{\sigma_{l_A}} \right)^2. \tag{39}$$

4. Results and Discussions

Following the aforementioned methodology, we carried out two sets of analysis: (A) we fit the whole parameter space composed by the Hubble constant H_0, the matter density parameter $\Omega_{m,0}$, γ and m; and (B) we set $H_0 = 67.37 \pm 0.54$ and $\Omega_{m,0} = 0.3147 \pm 0.0074$ which are the best fit values of joint analysis of the CMB power spectrum and other probes [10], while m and γ stay free to vary. All results are summarized in Table 2, and some comments are deserved.

In Analysis (A), we show that the best fit values of $[H_0, \Omega_{m,0}]$ are consistent with the most common cosmological analysis at low redshift, and $[m, \gamma]$ are compatible with the ones from [44,45] and their standard values at 1σ meaning that DE is well described by a cosmological constant. Interestingly, although our parameter space is larger than previous analysis, we get a comparable precision in m. This fact expresses the constraining powerful of this dataset with respect to the one used in previous analysis. The matter density is always compatible with current constraint from *Planck* 2018 results [10] at $\sim 2\sigma$. Nevertheless, there are two cases in which the central value of $\Omega_{m,0}$ gets closer to the one from *Planck* at $\sim 1\sigma$: (i) when using only $H(z)$ and CMB temperature data; and (ii) when using all datasets. In addition, the central value of the Hubble constant deserves some comments. When we used only $H(z)$ and T_{CMB} datasets, we obtained a lower central value of H_0 that is compatible at 1σ with *Planck* 2018 constraints and at 3σ with recent constraint from SNIa [94,95]. On the contrary, when introducing luminosity distances measurements, the best fits values of H_0 increases showing a

tension with *Planck* 2018 results. The agreement of H_0 from the expansion rate data is rather expected since it has been found in other recent analysis [96–98].

Table 2. Maximum likelihood parameters and 1σ uncertainties from the MCMC algorithm and for the following datasets.

Dataset	$[H_0, \Omega_{m,0}]$ Free			
	H_0	$\Omega_{m,0}$	m	γ
$H(z)+T_{CMB}$	$66.9^{+2.56}_{-2.34}$	$0.314^{+0.055}_{-0.045}$	$0.07^{+0.16}_{-0.14}$	1.34 ± 0.02
SNIa+$H(z)+T_{CMB}$	$71.02^{+0.85}_{-0.91}$	0.26 ± 0.03	0.01 ± 0.11	1.34 ± 0.02
SNIa+GRB+$H(z)+T_{CMB}$	$71.46^{+0.84}_{-0.85}$	0.25 ± 0.03	$0.03^{+0.10}_{-0.11}$	1.34 ± 0.02
SNIa+GRB+$H(z)$+BAO+T_{CMB}	$70.31^{+0.66}_{-0.62}$	0.30 ± 0.01	0.18 ± 0.06	1.36 ± 0.01
SNIa+GRB+$H(z)$+BAO+T_{CMB}+CMB	69.8 ± 0.6	0.29 ± 0.01	0.01 ± 0.02	1.335 ± 0.005
	$[H_0, \Omega_{m,0}] = [67.37, 0.315]$			
$H(z)+T_{CMB}$			0.08 ± 0.07	1.34 ± 0.01
SNIa+$H(z)+T_{CMB}$			0.05 ± 0.07	1.34 ± 0.01
SNIa+GRB+$H(z)+T_{CMB}$			$0.04^{+0.07}_{-0.08}$	1.34 ± 0.01
SNIa+GRB+$H(z)$+BAO+T_{CMB}			0.05 ± 0.06	1.339 ± 0.009
SNIa+GRB+$H(z)$+BAO+T_{CMB}+CMB			0.01 ± 0.02	1.332 ± 0.005

Interestingly, the central value of m in the analysis including all the background observables is higher and it is compatible with zero only at 3σ. In such case, the power law index is $m = 0.18 \pm 0.06$ which can be recast in term of the equation of state parameter using Equation (12) and obtaining $w_{eff} = -0.94 \pm 0.02$, which is in tension with latest results from Planck satellite ($w = -1.04 \pm 0.1$ [10]). This fact demands a deeper analysis to be done with forthcoming datasets such as LSST, Euclid and WFIRST which will explore the Universe until redshift $z \sim 6$ providing high redshift SNIa and BAO data, and growth factor data with unprecedented precision [99–102]. Finally, in the full analysis including also the CMB constraints, we found a lower value of m which can be translated in $w_{eff} = -0.996 \pm 0.007$, which is perfectly compatible with a cosmological constant. To compare the decaying DE model with ΛCMD, we applied the AIC criteria obtaining $\Delta(AIC) = 1.53$ which slightly favors the standard cosmological model over the decaying DE one.

In the second analysis, H_0 and $\Omega_{m,0}$ are fixed to the *Planck* 2018 best fit values, and the parameters m and γ are fully in agreement with their expected values. Our best constraint of the power law index is $m = 0.01 \pm 0.02$ which means $w_{eff} = -0.996 \pm 0.007$ fully compatible with *Planck* 2018 results, and with a cosmological constant at 1σ. Moreover, to directly compare our results with the ones in [44,45], we carried out another analysis setting $\gamma = 4/3$ and leaving only m as free parameter. The constrained values of m with 1σ error is: $m = 0.004 \pm 0.006$, which represents a factor of ~ 5 improvement in σ_m over previous constraints.

Finally, in Figures 2 and 3, we show the 68% and 95% confidence levels of the whole and reduced parameter space constrained with the full dataset. To avoid overcrowding, in Figure 2, we do not overplot the contours from the several combinations of the datasets listed in Table 2.
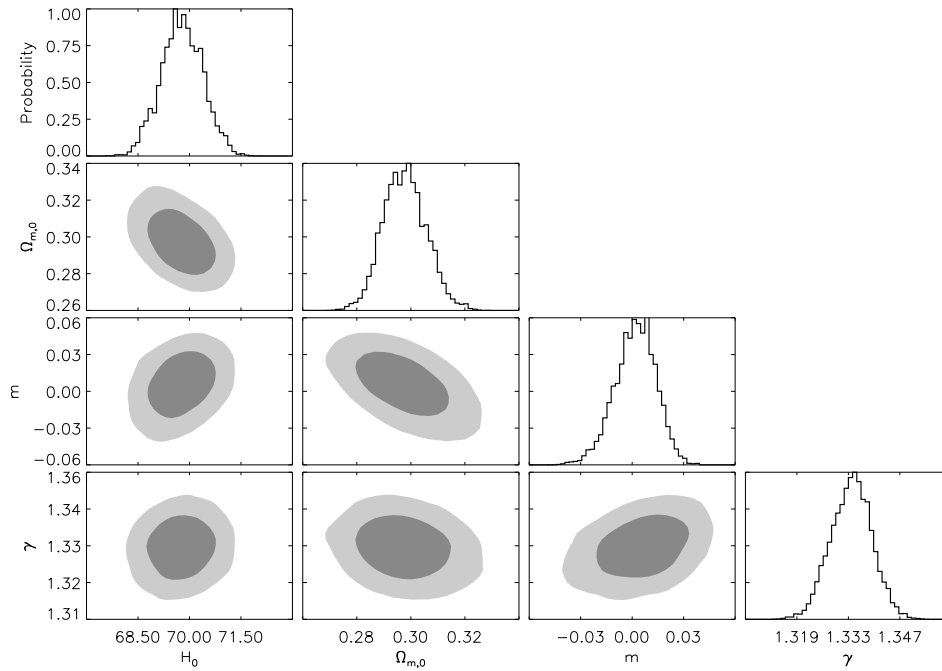
Figure 2. 2D marginalized contours of the model parameters $[H_0, \Omega_0, m, \gamma]$ obtained from the MCMC analysis. The 68% (dark grey) and 95% (light grey) confidence levels are shown for each pair of parameters. In each row, the marginalized likelihood distribution is also shown.
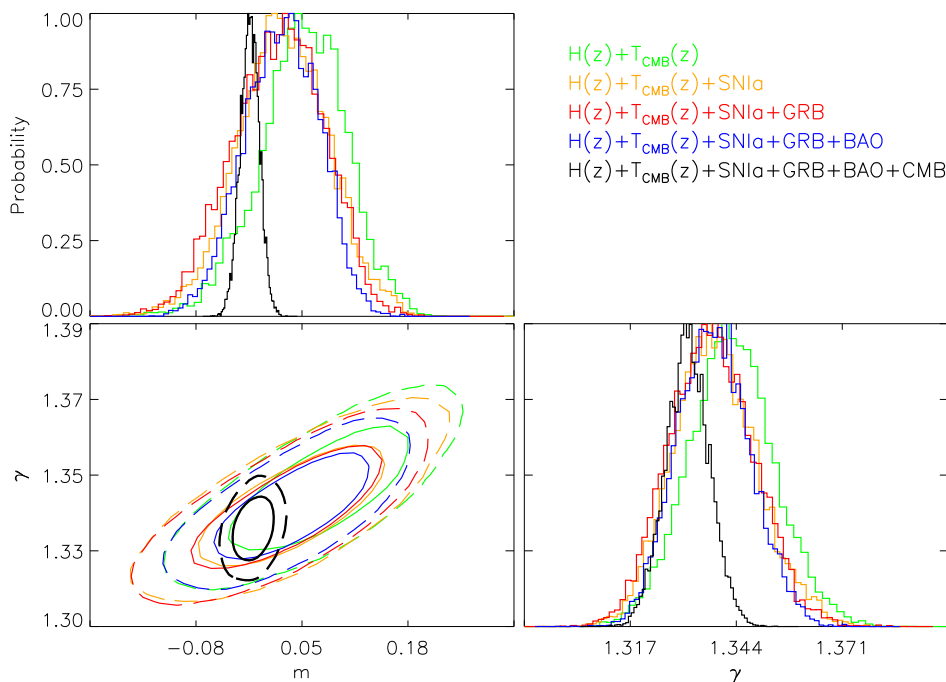

Figure 3. 2D marginalized 68% (solid line) and 95% (dashed line) contours of the model parameters $[m, \gamma]$ obtained from the MCMC analysis.

5. Conclusions

We have studied the decaying DE model introduced in [43–45]. In this model, photons and DM particles can be created or disrupted violating the conservation laws and altering the CMB

temperature–redshift scaling relation. The model has been studied using the latest dataset of SNIa, GRB, BAO, $H(z)$, $T_{CMB}(z)$ and *PlanckTT + lowP* data, which are described in Section 3.

First, we have explored the whole parameter space composed by the Hubble constant, the matter density fraction, and the parameters m and γ introduced in [44]. In this configuration, when using all the background observables, we obtain that the parameter m, which is the power law index of the DE decay law, is compatible with a cosmological constant only at 3σ. Therefore, forthcoming dataset could find a statistically relevant departure from standard cosmology, or alleviate this tension. Nevertheless, it is worth noting that, by adding the CMB constraints, such a tension disappears. Second, we have also studied a reduced parameter space composed by only m and γ, and setting the Hubble constant and the matter density parameter to their best fit values obtained recently by *Planck* satellite [10]. In this case, both parameters are always compatible at 1σ level with standard cosmology. Third, varying only m as in [44,45], we have improved the previous constraints of a factor ~ 5.

Finally, on the one side, we have demonstrated the improved constraining power of current dataset with respect to previous analysis, while, on the other side, we expect that forthcoming higher precision measurements of the CMB temperature at the location of high redshift galaxy clusters and Quasars, high redshift SNIa, improved measurements of BAO and of luminosity distance of GRBs, will be able to confirm or rule out decaying DE models [99–102].

Conflicts of Interest: The author declares no conflict of interest.

Abbreviations

The following abbreviations are used in this manuscript:

BAO	Baryon Acoustic Oscillation
DE	Dark Energy
DM	Dark Matter
FRW	Friedman–Robertson–Walker
GR	General Relativity
GRB	Gamma Ray Burst
MCMC	Monte Carlo Markov Chain
SNIa	Supernovae Type Ia
SPT	South Pole Telescope

References

1. Perlmutter, S.; Gabi, S.; Goldhaber, G.; Goobar, A.; Groom, D.E.; Hook, I.M.; Kim, A.G.; Kim, M.Y.; Lee, J.C.; Pain, R.; et al. Measurements of the Cosmological Parameters Omega and Lambda from the First Seven Supernovae at $z \geq 0.35$. *Astrophys. J.* **1997**, *483*, 565.
2. Riess, A.G.; Strolger, L.G.; Tonry, J.; Casertano, S.; Ferguson, H.C.; Mobasher, B.; Challis, P.; Filippenko, A.V.; Jha, S.; Li, W.; et al. Type Ia Supernova Discoveries at $z > 1$ from the Hubble Space Telescope: Evidence for Past Deceleration and Constraints on Dark Energy Evolution. *Astrophys. J.* **2004**, *607*, 665–687.
3. Astier, P.; Guy, J.; Regnault, N.; Pain, R.; Aubourg, E.; Balam, D.; Basa, S.; Carlberg, R.G.; Fabbro, S.; Fouchez, D.; et al. The Supernova Legacy Survey: Measurement of Ω_M, Ω_Λ and w from the first year data set. *Astron. Astrophys.* **2006**, *447*, 31–48.
4. Suzuki, N.; Rubin, D.; Lidman, C.; Aldering, G.; Amanullah, R.; Barbary, K.; Barrientos, L.F.; Botyanszki, J.; Brodwin, M.; Connolly, N.; et al. The Hubble Space Telescope Cluster Supernova Survey. V. Improving the Dark-energy Constraints above $z > 1$ and Building an Early-type-hosted Supernova Sample. *Astrophys. J.* **2012**, *746*, 85.

5.　Pope, A.C.; Matsubara, T.; Szalay, A.S.; Blanton, M.R.; Eisenstein, D.J.; Gray, J.; Jain, B.; Bahcall, N.A.; Brinkmann, J.; Budavari, T.; et al. Cosmological Parameters from Eigenmode Analysis of Sloan Digital Sky Survey Galaxy Redshifts. *Astrophys. J.* **2004**, *607*, 655.

6.　Percival, W.J.; Baugh, C.M.; Bland-Hawthorn, J.; Bridges, T.; Cannon, R.; Cole, S.; Colless, M.; Collins, C.; Couch, W.; Dalton, G.; et al. The 2dF Galaxy Redshift Survey: The power spectrum and the matter content of the Universe. *Mon. Not. R. Astron. Soc.* **2001**, *327*, 1297–1306.

7.　Tegmark, M.; Blanton, M.R.; Strauss, M.A.; Hoyle, F.; Schlegel, D.; Scoccimarro, R.; Vogeley, M.S.; Weinberg, D.H.; Zehavi, I.; Berlind, M.S.; et al. The Three-Dimensional Power Spectrum of Galaxies from the Sloan Digital Sky Survey. *Astrophys. J.* **2004**, *606*, 702.

8.　Hinshaw, G.; Larson, D.; Komatsu, E.; Spergel, D.N.; Bennett, C.L.; Dunkley, J.; Nolta, M.R.; Halpern, M.; Hill, R.S.; Odegard, N.; et al. Nine-Year Wilkinson Microwave Anisotropy Probe (WMAP) Observations: Cosmological Parameter Results. *Astrophys. J. Suppl. Ser.* **2013**, *208*, 19.

9.　Blake, C.; Kazin, E.A.; Beutler, F.; Davis, T.M.; Parkinson, D.; Brough, S.; Colless, M.; Contreras, C.; Couch, W.; Croom, S.; et al. The WiggleZ Dark Energy Survey: Mapping the distance-redshift relation with baryon acoustic oscillations. *Mon. Not. R. Astron. Soc.* **2011**, *418*, 1707.

10.　Planck Collaboration. Planck 2018 results. VI. Cosmological parameters. *arXiv* **2018**, arXiv:1807.06209.

11.　de Martino, I.; Génova-Santos, R.; Atrio-Barandela, F.; Ebeling, H.; Kashlinsky, A.; Kocevski, D.; Martins, C.J.A.P. Constraining the Redshift Evolution of the Cosmic Microwave Background Blackbody Temperature with PLANCK Data. *Astrophys. J.* **2015**, *808*, 128.

12.　De Martino, I.; Martins, C.J.A.P.; Ebeling, H.; Kocevski, D. Constraining spatial variations of the fine structure constant using clusters of galaxies and Planck data. *Phys. Rev. D* **2016**, *94*, 083008.

13.　Peebles, P.J.E.; Ratra, B. Cosmology with a time-variable cosmological 'constant'. *Astrophys. J. Lett.* **1988**, *325*, L17.

14.　Ratra, B.; Peebles, P.J.E. Cosmological consequences of a rolling homogeneous scalar field. *Phys. Rev. D* **1988**, *37*, 3406.

15.　Sahni, V.; Starobinsky, A.A. The Case for a Positive Cosmological Λ-Term. *Int. J. Mod. Phys.* **2000**, *D9*, 373. doi:10.1142/S0218271800000542

16.　Caldwell, R.R. A phantom menace? Cosmological consequences of a dark energy component with super-negative equation of state. *Phys. Lett. B* **2002**, *545*, 23.

17.　Padmanabhan, T. Cosmological constant-the weight of the vacuum. *Phys. Rep.* **2003**, *380*, 235.

18.　Peebles, P.J.E.; Ratra, B. The cosmological constant and dark energy. *Rev. Mod. Phys.* **2003**, *75*, 559.

19.　Demianski, M.; Piedipalumbo, E.; Rubano, C.; Tortora, C. Two viable quintessence models of the Universe: Confrontation of theoretical predictions with observational data. *Astron. Astrophys.* **2005**, *431*, 27.

20.　Cardone, V.F.; Tortora, C.; Troisi, A.; Capozziello, S. Beyond the perfect fluid hypothesis for the dark energy equation of state. *Phys. Rev. D* **2006**, *73*, 043508.

21.　Capolupo, A. Dark matter and dark energy induced by condensates. *Adv. High Energy Phys.* **2016**, *2016*, doi:10.1155/2016/8089142.

22.　Capolupo, A. Quantum vacuum, dark matter, dark energy and spontaneous supersymmetry breaking. *Adv. High Energy Phys.* **2018**, *2018*, doi:10.1155/2018/9840351.

23.　Kleidis, K.; Spyrou, N.K. A conventional approach to the dark energy concept. *Astron. Astrophys.* **2011**, *529*, A26.

24.　Kleidis, K.; Spyrou, N.K. A conventional form of dark energy. *J. Phys. Conf. Ser.* **2011**, *283*, 012018.

25.　Kleidis, K.; Spyrou, N.K. Polytropic dark matter flows illuminate dark energy and accelerated expansion. *Astron. Astrophys.* **2015**, *576*, A23.

26.　Kleidis, K.; Spyrou, N.K. Dark energy: The shadowy reflection of dark matter? *Entropy* **2016**, *18*, 94.

27.　Kleidis, K.; Spyrou, N.K. Cosmological perturbations in the ΛCDM-like limit of a polytropic dark matter model. *Astron. Astrophys.* **2017**, *606*, A116.

28.　Caldwell, R.; Kamionkowski, M. The Physics of Cosmic Acceleration. *Ann. Rev. Nuclear Part. Sci.* **2009**, *59*, 397.

29.　Wang, B.; Abdalla, E.; Atrio-Barandela, F.; Pavón, D. Dark Matter and Dark Energy Interactions: Theoretical Challenges, Cosmological Implications and Observational Signatures. *Rep. Prog. Phys.* **2016** , *79*, 9.

30.　Capozziello, S.; de Laurentis, M.; Francaviglia, M.; Mercadante, S. From Dark Energy & Dark Matter to Dark Metric. *Found. Phys.* **2009**, *39*, 1161.

31. Nojiri, S.; Odintsov, S.D. Unified cosmic history in modified gravity: From F(R) theory to Lorentz non-invariant models. *Phys. Rep.* **2011**, *505*, 59–144.

32. de Martino, I.; De Laurentis, M.; Capozziello, S. Constraining f(R) gravity by the Large Scale Structure. *Universe* **2015**, *1*, 123.

33. Nojiri, S.; Odintsov, S.D.; Oikonomou, V.K. Modified gravity theories on a nutshell: Inflation, bounce and late-time evolution. *Phys. Rep.* **2017**, *692*, 1–104.

34. Nojiri, S.; Odintsov, S.D. Introduction to modified gravity and gravitational alternative for dark energy. *Int. J. Geom. Meth. Mod. Phys.* **2007**, *4*, 115.

35. Capozziello, S.; De Laurentis, M. Extended Theories of Gravity. *Phys. Rep.* **2011**, *509*, 167.

36. Arraut, I. The graviton Higgs mechanism. *Europhys. Letter* **2015**, *111*, 61001.

37. Arraut, I.; Chelabi, K. Non-linear massive gravity as a gravitational σ-model. *Europhys. Letter* **2016**, *115*, 31001.

38. Arraut, I.; Chelabi, K. Vacuum degeneracy in massive gravity: Multiplicity of fundamental scales. *Mod. Phys. Lett. A* **2017**, *32*, 1750112

39. Lima, J.A.S. Thermodynamics of decaying vacuum cosmologies. *Phys. Rev. D* **1996**, *54*, 2571.

40. Lima, J.A.S.; Alcaniz, J.A.S. Flat Friedmann-Robertson-Walker cosmologies with adiabatic matter creation: kinematic tests. *Astron. Astrophys.* **1999**, *348*, 1.

41. Lima, J.A.S.; Silva, A.I.; Viegas, S.M. Is the radiation temperature-redshift relation of the standard cosmology in accordance with the data? *Mon. Not. R. Astron. Soc.* **2000**, *312*, 747.

42. Puy, D. Thermal balance in decaying Λ cosmologies. *Astron. Astrophys.* **2004**, *422*, 1–9.

43. Ma, Y. Variable cosmological constant model: The reconstruction equations and constraints from current observational data. *Nuclear Phys. B* **2008**, *804*, 262.

44. Jetzer, P.; Puy, D.; Signore, M.; Tortora, C. Limits on decaying dark energy density models from the CMB temperature-redshift relation. *Gen. Relat. Grav.* **2011**, *43*, 1083.

45. Jetzer, P.; Tortora, C. Constraints from the CMB temperature and other common observational data sets on variable dark energy density models. *Phys. Rev. D* **2011**, *84*, 043517.

46. Fixsen, D.J. The Temperature of the Cosmic Microwave Background. *Astrophys. J.* **2009**, *707*, 916.

47. Bahcall, J.N.; Wolf, R.A. Fine-Structure Transitions. *Astrophys. J.* **1968**, *152* , 701.

48. Fabbri, R.; Melchiorri, F.; Natale, V. The Sunyaev-Zel'dovich effect in the millimetric region. *Astrophys. Space Sci.* **1978**, *59*, 223.

49. Rephaeli, Y. On the determination of the degree of cosmological Compton distortions and the temperature of the cosmic blackbody radiation. *Astrophys. J.* **1980**, *241*, 858.

50. Sunyaev, R.A.; Zeldovich, Y.B. The Observations of Relic Radiation as a Test of the Nature of X-Ray Radiation from the Clusters of Galaxies. *Comment Astrophys. Space Phys.* **1972**, *4*, 173.

51. Avgoustidis, A.; Génova-Santos, R.T.; Luzzi, G.; Martins, C.J.A.P. Subpercent constraints on the cosmological temperature evolution. *Phys. Rev. D* **2016**, *93*, 043521.

52. Luzzi, G.; Shimon, M.; Lamagna, L.; Rephaeli, Y.; De Petris, M.; Conte, A.; De Gregori, S.; Battistelli, E. S. Redshift Dependence of the Cosmic Microwave Background Temperature from Sunyaev-Zeldovich Measurements. *Astrophys. J.* **2009**, *705* , 1122.

53. Luzzi, G.; Génova-Santos, R.T.; Martins, C.J.A.P.; De Petris, M.; Lamagna, L. Constraining the evolution of the CMB temperature with SZ measurements from Planck data. *J. Cosmol. Astropart. Phys.* **2015**, *1509*, 011.

54. Hurier, G.; Aghanim, N.; Douspis, M.; Pointecouteau, E. Measurement of the T_{CMB} evolution from the Sunyaev-Zel'dovich effect. *Astron. Astrophys.* **2014**, *561* , A143.

55. Saro, A.; Liu, J.; Mohr, J.J.; Aird, K.A.; Ashby, M.L.N.; Bayliss, M.; Benson, B.A.; Bleem, L.E.; Bocquet, S.; Brodwin, M.; et al. Constraints on the CMB temperature evolution using multiband measurements of the Sunyaev-Zel'dovich effect with the South Pole Telescope. *Mon. Not. R. Astron. Soc.* **2014**, *440*, 2610.

56. De Martino, I.; Atrio-Barandela, F.; da Silva, A.; Ebeling, H.; Kashlinsky, A.; Kocevski, D.; Martins, C.J.A.P. Measuring the Redshift Dependence of the Cosmic Microwave Background Monopole Temperature with Planck Data. *Astrophys. J.* **2012**, *757*, 144.

57. Weinberg, S. *Gravitation and Cosmology: Principles and Applications of the General Theory of Relativity;* Wiley: New York, NY, USA, 1972.

58. Hastings, W.K. Monte Carlo Sampling Methods using Markov Chains and their Applications. *Biometrika* **1970**, *57*, 97.

59. Metropolis, N.; Rosenbluth, A.W.; Rosenbluth, M.N.; Teller, A.H.; Teller, E. Equation of State Calculations by Fast Computing Machines. *J. Chem. Phys.* **1953**, *21*, 1087.
60. Gelman, A.; Roberts, G.O.; Gilks, W.R. Efficient Metropolis jumping rule. *Bayesian Stat.* **1996**, *5*, 599.
61. Roberts, G.O.; Gelman, A.; Gilks, W.R. Weak convergence and optimal scaling of random walk Metropolis algorithms. *Ann. Appl. Probab.* **1997**, *7*, 110.
62. Gelman, A.; Rubin, D.B. Inference from Iterative Simulation Using Multiple Sequences. *Stat. Sci.* **1992**, *7*, 457.
63. Spergel, D.N.; Verde, L.; Peiris, H.V.; Komatsu, E.; Nolta, M.R.; Bennett, C.L.; Halpern, M.; Hinshaw, G.; Jarosik, N.; Kogut, A.; et al. First-Year Wilkinson Microwave Anisotropy Probe (WMAP) Observations: Determination of Cosmological Parameters. *Astrophys. J. Suppl.* **2003**, *148*, 175.
64. Akaike, H. A new look at the statistical model identification. *IEEE Trans. Autom. Control* **1974**, *19*, 716.
65. Amanullah, R.; Lidman, C.; Rubin, D.; Aldering, G.; Astier, P.; Barbary, K.; Burns, M.S.; Conley, A.; Dawson, K.S.; Deustua, S.E.; et al. Spectra and Hubble Space Telescope Light Curves of Six Type Ia Supernovae at $0.511 < z < 1.12$ and the Union2 Compilation. *Astrophys. J.* **2010**, *716*, 712.
66. Di Pietro, E.; Claeskens, J.F. Future supernovae data and quintessence models. *Mon. Not. R. Astron. Soc.* **2003**, *341*, 1299.
67. Nesseris, S.; Perivolaropoulos, L. Comparison of the Legacy and Gold SnIa Dataset Constraints on Dark Energy Models. *Phys. Rev. D* **2005**, *72*, 123519.
68. Perivolaropoulos, L. Constraints on linear negative potentials in quintessence and phantom models from recent supernova data. *Phys. Rev. D* **2005**, *71*, 063503.
69. Wei, H. Constraints on linear negative potentials in quintessence and phantom models from recent supernova data. *Phys. Lett. B* **2010**, *687*, 286.
70. Luković, V.V.; D'Agostino, R.; Vittorio, N. Is there a concordance value for H_0? *Astron. Astrophys.* **2016**, *595*, A109.
71. Jimenez, R.; Loeb, A. Constraining Cosmological Parameters Based on Relative Galaxy Ages. *Astrophys. J.* **2005**, *573*, 37.
72. Simon, J.; Verde, L.; Jimenez, R. Constraints on the redshift dependence of the dark energy potential. *Phys. Rev. D* **2005**, *71*, 123001.
73. Stern, D.; Jimenez, R.; Verde, L.; Stanford, S.A.; Kamionkowski, M. Cosmic Chronometers: Constraining the Equation of State of Dark Energy. II. A Spectroscopic Catalog of Red Galaxies in Galaxy Clusters. *Astrophys. J. Suppl.* **2010**, *188*, 280.
74. Zhang, C.; Zhang, H.; Yuan, S.; Liu, S.; Zhang, T.J.; Sun, Y.C. Four new observational H(z) data from luminous red galaxies in the Sloan Digital Sky Survey data release seven. *Res. Astron. Astrophys.* **2014**, *14*, 1221.
75. Moresco, M. Raising the bar: New constraints on the Hubble parameter with cosmic chronometers at $z \sim 2$. *Mon. Not. R. Astron. Soc.* **2015**, *450*, L16.
76. Moresco, M.; Cimatti, A.; Jimenez, R.; Pozzetti, L.; Zamorani, G.; Bolzonella, M.; Dunlop, J.; Lamareille, F.; Mignoli, M.; Pearce, H.; et al. Improved constraints on the expansion rate of the Universe up to $z \sim 1.1$ from the spectroscopic evolution of cosmic chronometers. *J. Cosmol. Astropart. Phys.* **2012**, *2012*, 1112–1119.
77. Moresco, M.; Pozzetti, L.; Cimatti, A.; Jimenez, R.; Maraston, C.; Verde, L.; Thomas, D.; Citro, A.; Tojeiro, R.; Wilkinson, D. A 6% measurement of the Hubble parameter at $z \sim 0.45$: Direct evidence of the epoch of cosmic re-acceleration. *J. Cosmol. Astropart. Phys.* **2016**, *2016*, 014.
78. Moresco, M.; Verde, L.; Pozzetti, L.; Jimenez, R.; Cimatti, A. New constraints on cosmological parameters and neutrino properties using the expansion rate of the Universe to $z \sim 1.75$. *J. Cosmol. Astropart. Phys.* **2012**, *2012*, 053.
79. Eisenstein, D.J.; Hu, W.; Tegmark, M. Cosmic Complementarity: H_0 and Ω_m from Combining Cosmic Microwave Background Experiments and Redshift Surveys. *Astrophys. J. Lett.* **1998**, *504*, L57.
80. Eisenstein, D.J.; Zehavi, I.; Hogg, D.W.; Scoccimarro, R.; Blanton, M.R.; Nichol, R.C.; Scranton, R.; Seo, H.; Tegmark, M.; Zheng, Z.; et al. Detection of the Baryon Acoustic Peak in the Large-Scale Correlation Function of SDSS Luminous Red Galaxies. *Astrophys. J.* **2005**, *633*, 560.
81. Beutler, F.; Blake, C.; Colless, M.; Jones, D.H.; Staveley-Smith, L.; Campbell, L.; Parker, Q.; Saunders, W.; Watson, F. The 6dF Galaxy Survey: baryon acoustic oscillations and the local Hubble constant. *Mon. Not. R. Astron. Soc.* **2011**, *416*, 3017.
82. Ross, A.J.; Samushia, L.; Howlett, C.; Percival, W.J.; Burden, A.; Manera, M.; The clustering of the SDSS DR7 main Galaxy sample - I. A 4 per cent distance measure at $z = 0.15$. *Mon. Not. R. Astron. Soc.* **2015**, *449*, 835.

83. Anderson, L.; Aubourg, E.; Bailey, S.; Beutler, F.; Bhardwaj, V.; Blanton, M.; Bolton, A.S.; Brinkmann, J.; Brownstein, J.R.; Burden, A.; et al. The clustering of galaxies in the SDSS-III Baryon Oscillation Spectroscopic Survey: baryon acoustic oscillations in the Data Releases 10 and 11 Galaxy samples. *Mon. Not. R. Astron. Soc.* **2014**, *441*, 24.

84. Delubac, T.; Bautista, J.E.; Busca, N.G.; Rich, J.; Kirkby, D.; Bailey, S.; Font-Ribera, A.; Slosar, A.; Lee, K.G.; Pieri, M.M.; et al. Baryon acoustic oscillations in the Lyα forest of BOSS DR11 quasars. *Astron. Astrophys.* **2015**, *574*, A59.

85. Font-Ribera, A.; Kirkby, D.; Busca, N.; Miralda-Escudé, J.; Ross, N.P.; Slosar, A.; Rich, J.; Aubourg, E.; Bailey, S.; Bhardwaj, V.; et al. Quasar-Lyman α forest cross-correlation from BOSS DR11: Baryon Acoustic Oscillations. *J. Cosmol. Astropart. Phys.* **2014**, *5*, 27.

86. Wei, H. Observational constraints on cosmological models with the updated long gamma-ray bursts. *J. Cosmol. Astropart. Phys.* **2010**, *1008*, 020.

87. Haridasu, B.S.; Luković, V.V.; D'Agostino, R.; Vittorio, N. Strong evidence for an accelerating Universe. *Astron. Astrophys.* **2017**, *600*, L1.

88. Amati, L.; Frontera, F.; Guidorzi, C. Extremely energetic Fermi gamma-ray bursts obey spectral energy correlations. *Astron. Astrophys.* **2009**, *508*, 173.

89. Amati, L.; Frontera, F.; Tavani, M.; in't Zand, J.J.M.; Antonelli, A.; Costa, E.; Feroci, M.; Guidorzi, C.; Heise, J.; Masetti, N.; et al. Intrinsic spectra and energetics of BeppoSAX Gamma-Ray Bursts with known redshifts. *Astron. Astrophys.* **2002**, *390*, 81.

90. Amati, L.; Guidorzi, C.; Frontera, F.; Della Valle, M.; Finelli, F.; Landi, R.; Montanari, E. Measuring the cosmological parameters with the $E_{p,i} - E_{iso}$ correlation of gamma-ray bursts. *Mon. Not. R. Astron. Soc.* **2008**, *391*, 577.

91. Kosowsky, A.; Milosavljevic, M.; Jimenez, R. Efficient cosmological parameter estimation from microwave background anisotropies. *Phys. Rev. D* **2002**, *66*, 063007.

92. Wang, Y.; Mukherjee, P. Observational Constraints on Dark Energy and Cosmic Curvature. *Phys. Rev. D* **2007**, *76*, 103533.

93. Planck Collaboration. Planck 2015 results. XIV. Dark energy and modified gravity. *Astron. Astrophys.* **2016**, *594*, A14.

94. Riess, A.G.; Macri, L.M.; Hoffmann, S.L. A 2.4% Determination of the Local Value of the Hubble Constant. *Astrophys. J.* **2016**, *826*, 56.

95. Riess, A.G.; Casertano, S.; Yuan, W.; Macri, L.; Anderson, J.; MacKenty, J.W.; Bowers, J.B.; Clubb, K.I.; Filippenko, A. V.; Jones, D.O.; et al. New Parallaxes of Galactic Cepheids from Spatially Scanning the Hubble Space Telescope: Implications for the Hubble Constant. *arXiv* **2018**, arXiv:1801.01120.

96. Yu, H.; Ratra, B.; Wang, F.Y. Hubble Parameter and Baryon Acoustic Oscillation Measurement Constraints on the Hubble Constant, the Deviation from the Spatially Flat ΛCDM Model, the Deceleration-Acceleration Transition Redshift, and Spatial Curvature. *Astrophys. J.* **2018**, *856*, 3.

97. Gómez-Valent, A.; Amendola, L. H_0 from cosmic chronometers and Type Ia supernovae, with Gaussian Processes and the novel Weighted Polynomial Regression method. *J. Cosmol. Astropart. Phys.* **2018**, *2018*, 051.

98. Wang, D.; Zhang, W. Machine Learning Cosmic Expansion History. *arXiv* **2018**, arXiv:1712.09208.

99. LSST Science Collaborations and LSST Project. *LSST Science Book*, 2nd ed; LSST Science Collaborations and LSST Project: Tucson, AZ, USA, 2009; arXiv:0912.0201.

100. Laureijs, R.; Amiaux, J.; Arduini, S.; Auguères, J.L.; Brinchmann, J.; Cole, R.; Cropper, M.; Dabin, C.; Duvet, L.; Ealet, A.; et al. Euclid Definition Study Report ESA/SRE(2011)12. *arXiv* **2011**, arXiv:1110.3193.

101. Spergel, D.; Gehrels, N.; Baltay, C.; Bennett, D.; Breckinridge, J.; Donahue, M.; Dressler, A.; Gaudi, B.S.; Greene, T.; Guyon, O.; et al. Wide-Field InfrarRed Survey Telescope-Astrophysics Focused Telescope Assets WFIRST-AFTA 2015 Report. *arXiv* **2015**, arXiv:1503.03757.

102. Kashlinsky, A.; Arendt, R.G.; Atrio-Barandela, F.; Helgason, K. Lyman-tomography of cosmic infrared background fluctuations with Euclid: Probing emissions and baryonic acoustic oscillations at $z > 10$. *Astrophys. J. Lett.* **2015**, *813*, L12.